IEEE Access
Multidisciplinary | Rapid Review | Open Access Journal

Digital Object Identifier 10.1109/ACCESS.2021.DOI

Linearized versus nonlinear observability analysis for Lithium-ion battery dynamics: why respecting the nonlinearities is key for proper observer design

ANIRUDH ALLAM[1], (Graduate Student Member, IEEE), AND SIMONA ONORI[1], (Senior Member, IEEE)

[1]Energy Resources Engineering Department, Stanford University, Stanford, California 94305, USA

Corresponding author: Simona Onori (e-mail: sonori@stanford.edu).

ABSTRACT Electrochemical model-based observers for battery state estimation play an important role in advanced battery management system design to provide accurate real-time estimates of unmeasurable critical internal variables. In this work, the observability of an electrochemical battery model is studied through a thorough nonlinear observability analysis to quantify the measure of observability, and therefore the quality of estimated variables, by accounting for the rank and the condition number of the observability matrix. The paper highlights the need for nonlinear observability analysis instead of a linearized analysis, and the practical aspects of the electrochemical model's observability are investigated and quantified for different input conditions, electrode's chemistry, and discretization grid points.

INDEX TERMS battery state estimation, condition number test, lithium-ion battery, nonlinear observability analysis, rank test, single particle model.

NOMENCLATURE

A	Cell cross sectional area [m^2].
$D_{s,j}$	Solid phase diffusion [m^2/s].
F	Faraday's constant [C/mol].
I_{batt}	Applied current [A].
$\kappa(\mathcal{O})$	Condition number of matrix $\mathcal{O}$.
L_j	Domain thickness [m].
L_{sei}	SEI layer thickness [m].
M_{sei}	Molar mass of SEI layer [kg/mol].
N	Number of radial discretization grids.
$\mathcal{O}$	Observability matrix.
R_g	Universal gas constant [J/mol-K].
R_j	Particle radius [m].
R_l	Lumped resistance [Ω].
T_{ref}	Reference temperature [^{o}C].
U_j	Open circuit potential [V].
$a_{s,j}$	Specific interfacial surface area [m^{-1}].
$c_{e,0}$	Average electrolyte phase concentration [mol/m^3].
$c_{s,j}$	Solid phase concentration [mol/m^3].
$c_{s,j,surf}$	Surface concentration [mol/m^3].
$c_{s,j,max}$	Maximum solid phase concentration [mol/m^3].
$i_{0,j}$	Exchange current density [A/m^2].
$i_{int,j}$	Intercalation current density [A/m^2].
k_j	Reaction rate constant [$m^{2.5}$/s-$mol^{0.5}$].
n	Size of the state vector.
r	Radial coordinate.
t	Temporal coordinate.
u	Input to the state-space system.
x	State vector.
y	Output of the state-space system.
α_a	Anodic transfer coefficient.
α_c	Cathodic transfer coefficient.
ϵ_j	Active volume fraction of solid phase.
η_j	Overpotential [V].
Subscript j	Refers to negative or positive electrode.
Subscript n	Refers to negative electrode.
Subscript p	Refers to positive electrode.

I. INTRODUCTION

THE growing market of lithium-ion batteries in consumer electronics, automobiles, unmanned aerial vehicles, and power grid sector grids has stressed the need and relevance for a properly designed advanced Battery Management System (BMS) that can ensure the battery's reliability and performance [1]. One of the key aspects of an advanced BMS is monitoring critical battery variables of interest such as State of Charge (SOC) and State of Health (SOH) [2]–[4], which remain non-measurable via sensors, and use this information to devise on-line control strategies to utilize the batteries safely and effectively. The BMS relies on model-based or data-driven estimation algorithms to "observe" these unmeasurable variables [5]. In the case of model-based estimation, the algorithm uses available input/output sensor information (current, voltage, and temperature) along with a mathematical representation of the battery to estimate, as accurately as possible, the internal battery state variables [6]. The accuracy of these estimates, however, largely depends on the accuracy and fidelity of the battery model [1]. The very first on-line BMS algorithms were relying on empirical and highly calibrated equivalent circuit battery models [6], [7], whereas the latest trend is to rely on the more accurate electrochemical dynamics of the battery to retain relevant physics for accurate state estimation [1]. Consequently, the choice of models has largely gravitated from empirical equivalent circuit models towards physics-based electrochemical models that are capable of capturing the battery behavior more accurately.

A. RELATED LITERATURE

Plenty of research has been carried out on electrochemical model-based closed-loop observers/estimators that estimate the battery internal states [8]–[18], such as the solid phase lithium concentration from which the battery SOC is then derived. The first step towards developing a model-based observer for any dynamic system is to verify the observability property of the model. This property corroborates if there exists a relationship between the model states to be estimated and the available input/output measurements. Hence, it follows that observability of a system is a property that guarantees that its internal states can be uniquely inferred based on available measurements.

In one of the earliest defining works on battery state estimation, the issues with observability in an electrochemical model are discussed and attributed to the peculiar structure of the output voltage equation, which led to weak observability when estimating the individual lithium concentration in the positive and negative electrode [9]. In order to overcome the issues of weak observability, different methods to estimate the lithium concentration in a single electrode or both electrodes were presented in the literature ranging from imposing an algebraic constraint on lithium conservation [9], single electrode observers [12], inclusion of thermal model and measurements [15], and interconnected observers [16]. *Despite the abundance of such electrochemical model-based closed-loop observers, there is only a fleeting emphasis on the observability analysis of this model. Clearly, the weak observability of the electrochemical model is taken for granted, and there has been no attempt to delve deep and present a thorough observability analysis for different conditions such as zero current, constant current, and dynamic current input scenarios.* In addition, it is neither apparent nor has it been reported in the literature how the observability of this model changes based on the positive electrode's chemistry, which can alter the steepness or flatness of the nonlinearities in the output voltage equation. Further, the electrochemical model is characterized by Partial Differential Equations (PDEs) which are discretized into a system of Ordinary Differential Equations (ODEs) for developing observers. Hence, it is paramount to understand how the observability property remains the same or deteriorates as the number of discretization grid points change causing the sparsity of the system to increase.

Evidently so, there is a need for a detailed observability analysis of a nonlinear electrochemical model. In the literature, observability analysis has been carried out on a linearized electrochemical model [19], however, it is understood that the nonlinear observability analysis at an operating point is not the same as the observability of the linearized system around that operating point [20]. More importantly, nonlinear observability analysis takes the system inputs and its derivatives into account, as opposed to the analysis for linear or linearized systems [21], [22]. Neglecting the effect of input renders the observability analysis on linearized systems to be incomplete, and therefore inadequate. Hence, the proper evaluation of observability analysis/observer design for nonlinear battery system over its linearized dynamics is preferred.

Generally speaking, observability analysis, traditionally, has been accompanied with the rank test of the observability matrix in both, linear and nonlinear, systems. It is understood that the rank test verifies whether the system is observable or not, but does not comment on the quality of the observability. Studies have shown that the condition number of the observability matrix is key to determining the quality of the estimated internal states [12], [23]–[25]. There are situations where the system is deemed observable but the quality of the estimates could be poor enough to not warrant an observer design, which, as it will be revealed in the following sections, is the case with the electrochemical model when estimating the lithium concentration in both electrodes.

B. CONTRIBUTIONS

From Section I-A, it emerges that there is a gap to be addressed with respect to carrying out a thorough nonlinear observability analysis of an electrochemical model. To that end, this work aims to contribute to the existing literature by (i) presenting a holistic nonlinear observability analysis by taking into consideration the rank test and the condition number, (ii) demonstrating that the nonlinear observability analysis of electrochemical model carries more information

than its linearized observability analysis counterpart, (iii) evaluating the observability for different electrode chemistry, (iv) evaluating the observability for diverse input conditions (such as zero current and constant current of differing magnitudes), and (v) studying the effect on observability due to PDE to ODE spatial discretization grid points. In addition, the improvement in observability brought about by implementing an alternate observer design structure, such as the novel interconnected observer [16], [17], is studied and recommendations regarding the order of model-based observers and future research directions are discussed.

C. OUTLINE

The remainder of this paper is organized as follows. In Section II, the notations used in this paper are laid out. In Section IV, the governing equations describing the electrochemical model and its state space representation are presented. Section III introduces the notion of observability for nonlinear systems and discusses the rank and condition number to determine the quality of observability. In Section V, the nonlinear observability analysis of the electrochemical is described. Section VI presents the results of the nonlinear observability analysis and discusses the dependency of the observability on input current conditions and positive electrode's chemistry and highlights the difference between nonlinear observability analysis and linearized observability analysis. Moreover, the observability issues with estimating lithium concentration in both electrodes is emphasized and the improvement in observability brought about by a choice of observer from the literature, in the form of an interconnected observer, is presented. This is followed by the discussion reflecting on the impact and outlook of the presented work in Section VII and the conclusions in Section VIII.

II. PRELIMINARIES

The following notations and symbols are used in the paper:

- $||\cdot||$ is the Euclidean norm; for a square matrix $A \in \mathbb{R}^{n\times n}$, the Euclidean norm is $||A|| = \sqrt{\sum_{p=1}^{n}\sum_{q=1}^{n}(a_{pq})^2}$, where a_{pq} are the elements of the matrix A, and p, q refer to the rows and columns of the matrix.
- The gradient of a scalar function $h(x) : R^n \to R$ is $\dfrac{\partial h}{\partial x}$, denoted as ∇h.
- Subscript j denotes the domain in the lithium-ion battery, negative (n) or positive electrode (p), $j \in [n, p]$.

Definition 1: Let $h : R^n \to R$ be a smooth scalar function and $f : R^n \to R$ be a smooth vector field, then the Lie derivative of h with respect to f is a scalar function interpreted as differentiation of function h in the direction of the vector f defined as

$$L_f(h) = \nabla h f. \tag{1}$$

Definition 2: For any general nonlinear system given by

$$\begin{aligned} \dot{x} &= f(x,u) \\ y &= h(x,u), \end{aligned} \tag{2}$$

where $h : R^n \times R \to R$ and $f : R^n \times R \to R$, the derivatives of the output can be represented using Lie derivatives as

$$\begin{cases} y = L_f^0(h) & = h(x,u) \\ \dot{y} = L_f^1(h) & = \dfrac{\partial L_f^0(h)}{\partial x}\dfrac{dx}{dt} + \dfrac{\partial L_f^0(h)}{\partial u}\dfrac{du}{dt} \\ \ddot{y} = L_f^2(h) & = \dfrac{\partial L_f^1(h)}{\partial x}\dfrac{dx}{dt} + \dfrac{\partial L_f^1(h)}{\partial u}\dfrac{du}{dt} + \dfrac{\partial L_f^1(h)}{\partial \dot{u}}\dfrac{d^2u}{dt^2} \\ \vdots \end{cases} \tag{3}$$

III. OBSERVABILITY OF NONLINEAR SYSTEMS

In this work, we consider a class of dynamics systems, which is linear in its states and nonlinear in the output, of the form

$$\begin{cases} \dot{x} & = f(x,u) = Ax + Bu \\ y & = h(x,u), \end{cases} \tag{4}$$

where $x \in \mathbb{R}^n$ denotes the internal system state variables, $u \in \mathbb{R}^p$ denotes the inputs to the system, $y \in \mathbb{R}^m$ are the system outputs, and h is a smooth continuous nonlinear function.

Definition 3: The system in (4) is locally weakly observable at x_0 if there exists a neighborhood D containing x_0 such that for every state $x_1 \in D$ (where $x_0 \neq x_1$), the inequality $h(x_0, u) \neq h(x_1, u)$ holds true for some finite $t > 0$.

Definition 4: The system is locally weakly observable if it is locally weakly observable for all initial states.

Remark 1: For the nonlinear system given in (4), the derivatives of the output can be represented using the Lie derivatives as given in (5).

A. RANK TEST

Observability is a fundamental structural property of the system that guarantees that the initial internal states of a system can be reconstructed based on input and output sensor measurements. It follows that if a system is observable, then the internal state variables can indeed be estimated using the input and output measurements, and an observer is designed for the system. The standard approach to address nonlinear observability utilizes constructs from differential geometry to check the rank condition as introduced in [21].

Theorem 1: [21] The system (4) is locally weakly observable at x_0 if

$$rank\,(\mathcal{O}) = n, \tag{6}$$

$$\begin{bmatrix} y \\ \frac{dy}{dt} \\ \frac{d^2y}{dt^2} \\ \vdots \end{bmatrix} = \begin{bmatrix} h(x,u) \\ \frac{\partial h}{\partial x}\frac{dx}{dt} + \frac{\partial h}{\partial u}\frac{du}{dt} \\ \frac{\partial \left(\frac{\partial h}{\partial x}\frac{dx}{dt} + \frac{\partial h}{\partial u}\frac{du}{dt}\right)}{\partial x}\frac{dx}{dt} + \frac{\partial \left(\frac{\partial h}{\partial x}\frac{dx}{dt} + \frac{\partial h}{\partial u}\frac{du}{dt}\right)}{\partial u}\frac{du}{dt} \\ \vdots \end{bmatrix}$$

$$= \begin{bmatrix} L_f^0(h) \\ L_f^1(h) \\ L_f^2(h) \\ \vdots \end{bmatrix} = \begin{bmatrix} L_f^0(h) \\ \frac{\partial L_f^0(h)}{\partial x}(Ax+Bu) + \frac{\partial L_f^0(h)}{\partial u}\dot{u} \\ \frac{\partial L_f^1(h)}{\partial x}(Ax+Bu) + \frac{\partial L_f^1(h)}{\partial u}\dot{u} + \frac{\partial L_f^1(h)}{\partial \dot{u}}\ddot{u} \\ \vdots \end{bmatrix}. \tag{5}$$

where $\mathcal{O}$ is a matrix constructed from the gradient of the $n-1$ Lie derivatives evaluated at x_0 given by

$$\mathcal{O} = \frac{d}{dx}\begin{bmatrix} L_f^0(h) \\ L_f^1(h) \\ \vdots \\ L_f^{n-1}(h) \end{bmatrix}_{x_0}. \tag{7}$$

B. CONDITION NUMBER TEST

The observability rank test essentially determines whether the system is weakly locally observable. However, it does not inform about the accuracy or quality of the estimates. To that end, the condition number of the observability matrix is considered as a measure of the system's observability, which quantifies the quality of estimates that can be inferred from the input and output measurement data. The condition number at a given operating point x_0 is given by

$$\kappa(\mathcal{O}) = ||\mathcal{O}^{-1}||||\mathcal{O}||. \tag{8}$$

In general, the condition number of a matrix indicates how poorly conditioned and close to being singular the matrix is. Therefore, a high condition number indicates that the errors in measurements are amplified and result in state estimates with large errors.

IV. BATTERY ELECTROCHEMICAL MODEL

In this work, a Single Particle Model (SPM) is chosen as the electrochemical dynamic representation of the a lithium-ion battery cell, as shown in Fig. 1. The SPM is a reduced-order physics-based electrochemical model that approximates its electrodes as spherical particles, assumes uniform current distribution, and neglects electrolyte dynamics, thereby attaining a trade-off between computational complexity and accuracy, hence making it suitable for real-time observer and controller design. In this section, the SPM governing laws describing the battery dynamics and its subsequent state space representation are detailed.

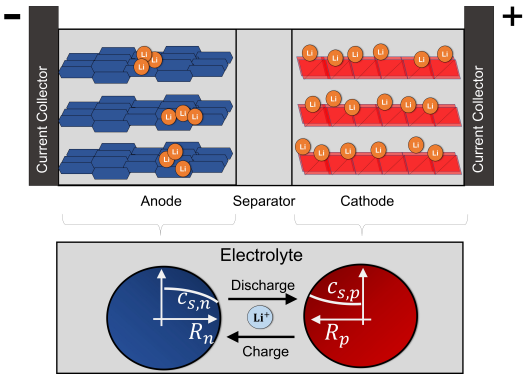

FIGURE 1: Schematic of a Single Particle Model with both its electrodes represented as spherical particles each.

A. GOVERNING EQUATIONS

The diffusion dynamics of lithium resulting due to the concentration gradient within the solid phase ($j \in [p,n]$) is given by Fick's law as

$$\frac{\partial c_{s,j}}{\partial t} = D_{s,j}\left[\frac{2}{r}\frac{\partial c_{s,j}}{\partial r} + \frac{\partial^2 c_{s,j}}{\partial r^2}\right], \tag{9}$$

where t and r are the temporal and radial coordinates, respectively, $j \in [p,n]$ represents the positive or negative electrode, $c_{s,j}$ is the lithium ion concentration in the solid phase of each electrode, and $D_{s,j}$ is the diffusion coefficient. The Neumann boundary conditions for the above Partial Differential Equation (PDE) are defined for the concentration at the center ($r = 0$) and the surface ($r = R_j$) of the solid phase (where R_j is the radius of the spherical particle). The flux of lithium ions at the center is zero, and the flux at the surface is equal to the rate at which lithium ions are being transported between the solid and electrolyte phase as described below:

$$\frac{\partial c_{s,j}}{\partial r}\Big|_{r=0} = 0 \quad \frac{\partial c_{s,j}}{\partial r}\Big|_{r=R_j} = \pm\frac{I_{batt}}{Fa_{s,j}D_{s,j}AL_j},$$

where I_{batt} is the battery current, F is Faraday's constant, A is the cell cross-sectional area, L_j is the electrode thickness, and $a_{s,j}$ is the electrode electroactive surface area.

In lithium-ion batteries, the intercalation/de-intercalation reactions occur at the surface of the particle, which induces a charge transfer at the solid-electrolyte interface. In electrochemistry, this kind of interfacial charge transfer is assumed to obey the Butler-Volmer equation, which describes the rate of the reaction. The Butler-Volmer equation is expressed as

$$i_{int,j} = i_{0,j}\left[\exp\left(\frac{\alpha_a F\eta_j}{R_g T}\right) - \exp\left(\frac{\alpha_c F\eta_j}{R_g T}\right)\right], \quad (10)$$

which relates the intercalation current density $i_{int,j}$ at an electrode to the overpotential η_j and the lithium concentration in the solid and electrolyte phase. Assuming the same anodic and cathodic transfer coefficients ($\alpha_a = \alpha_c = 0.5$), and uniform distribution of applied current into each electrode $\left(i_{int,j} = \frac{I_{batt}}{a_{s,j}AL_j}\right)$, the approximated Butler-Volmer equation allows the overpotential of each electrode to be modeled as

$$\eta_j = \frac{R_g T}{0.5F}\sinh^{-1}\left(\frac{I_{batt}}{2a_{s,j}AL_j i_{0,j}}\right), \quad (11)$$

where $i_{0,j} = Fk\sqrt{c_{e,0}c_{s,j,surf}\left(c_{s,j,max} - c_{s,j,surf}\right)}$ is the exchange current density, R_g is the universal gas constant, $c_{e,0}$ is the average electrolyte concentration, $c_{s,j,max}$ and $c_{s,j,surf}$ are the maximum solid phase concentration and surface concentration of both electrodes, respectively.

The equation for the terminal voltage of the battery is then given by

$$V = U_p\left(c_{s,p,surf}\right) + \eta_p\left(c_{s,p,surf}, I_{batt}\right) - U_n\left(c_{s,n,surf}\right) - \eta_n\left(c_{s,n,surf}, I_{batt}\right) - I_{batt}R_l \quad (12)$$

where R_l is the lumped contact resistance and U_j is the open circuit potential of each electrode as a function of their respective surface concentration.

B. STATE SPACE MODEL

The PDE describing the solid phase diffusion in (9) is radially discretized into $N+1$ concentration nodes via Finite Difference Method (FDM) to obtain a system of coupled ODEs, which are presented as a general state space model for the ease of understanding and numerical implementation. Let $x = [x_1, x_2]^T \in \mathbb{R}^{2N}$ be the state vector, $u = I_{batt}$ be the input current, and $y = V$ be the output voltage of the model. The state variables represent lithium concentration in the discretized nodes of positive and negative electrode, $x_1 = [c_{s,p,1}, c_{s,p,2}, \ldots, c_{s,p,N}]^T$ and $x_2 = [c_{s,n,1}, c_{s,n,2}, \ldots, c_{s,n,N}]^T$, respectively. Moreover, the surface concentration in both electrodes is given as $x_{1,N} = c_{s,p,surf}, x_{2,N} = c_{s,n,surf}$, respectively. Finally, the state space formulation is

$$\begin{aligned}\dot{x}_1(t) &= A_{11}x_1(t) + B_1 u(t)\\ \dot{x}_2(t) &= A_{22}x_2(t) + B_2 u(t)\\ y(t) &= U_p\left(x_{1,N}\right) + \eta_p\left(x_{1,N}, u\right) - U_n\left(x_{2,N}\right) - \\ &\quad \eta_n\left(x_{2,N}, u\right) - R_l u,\end{aligned} \quad (13)$$

where the elements of the matrices $A_{11}, A_{22} \in \mathbb{R}^{N\times N}$ are the coefficients of the concentration states and the elements of the column vectors $B_1, B_2 \in \mathbb{R}^{N\times 1}$ are coefficients of the input current, described below

$$A_{11} = \frac{D_{s,p}}{\Delta_r^2}\begin{bmatrix} -2 & 2 & 0 & \cdots & 0 & 0\\ 1/2 & -2 & 3/2 & \cdots & 0 & 0\\ \vdots & \vdots & \vdots & \ddots & \vdots & \vdots\\ 0 & 0 & 0 & \cdots & 2 & -2\end{bmatrix} \quad (14)$$

$$B_1 = \frac{-2}{\Delta_r F a_{s,p} A L_p}\begin{bmatrix} 0\\ 0\\ \vdots\\ \frac{N+1}{N}\end{bmatrix}$$

$$A_{22} = \frac{1}{\Delta_r^2}\begin{bmatrix} -2 & 2 & 0 & \cdots & 0 & 0\\ 1/2 & -2 & 3/2 & \cdots & 0 & 0\\ \vdots & \vdots & \vdots & \ddots & \vdots & \vdots\\ 0 & 0 & 0 & \cdots & 2 & -2\end{bmatrix}$$

$$B_2 = \frac{2}{\Delta_r F a_{s,n} A L_n}\begin{bmatrix} 0\\ 0\\ \vdots\\ \frac{N+1}{N}\end{bmatrix}.$$

Note that the state space model is linear in states but nonlinear in the output expression. The linearity follows from the assumption that the transport parameters in the solid phase are assumed to be constant and not varying with respect to concentration or temperature. The nonlinearity in the output is due to the open circuit potential of both electrodes, $U_p\left(x_{1,N}\right)$ and $U_n\left(x_{2,N}\right)$, which are a nonlinear function of their respective surface concentrations, and the overpotential of both electrodes, $\eta_p\left(x_{1,N}, u\right)$ and $\eta_n\left(x_{2,N}, u\right)$, which have a nonlinear relationship with the respective surface concentrations and the input battery current.

Remark 2: For the ease of presentation, henceforth, the variable n refers to the size of the battery state vector $x \in R^n$, where $n = 2N$.

V. NONLINEAR OBSERVABILITY ANALYSIS OF SPM

The SPM given in (13) is considered for a complete nonlinear observability analysis (in accordance with (5)) by evaluating the observability matrix via rank and condition number tests. The analysis will inform whether a SPM based observer is weakly locally observable and if it can estimate the solid-phase lithium concentration $x \in \mathbb{R}^n$, in both the positive and negative electrode, from the input current $u \in \mathbb{R}$ and output cell voltage $y \in \mathbb{R}$ measurements.

To construct the observability matrix, the Lie derivatives of the nonlinear output function of the SPM is considered. The 0^{th} Lie derivative of the SPM output is given by

$$\begin{aligned} L_f^0(h) &= h(x,u) \\ &= U_p(x_{1,N}) + \eta_p(x_{1,N},u) - U_n(x_{2,N}) + \\ &\quad \eta_n(x_{2,N},u) - R_l u. \end{aligned} \tag{15}$$

The 1^{st} Lie derivative is

$$\begin{aligned} L_f^1(h) &= \frac{\partial h(x,u)}{\partial x}\dot{x} + \frac{\partial h(x,u)}{\partial u}\dot{u} \\ &= \frac{\partial h(x,u)}{\partial x_{1,1}}\dot{x}_{1,1} + \ldots + \frac{\partial h(x,u)}{\partial x_{1,N}}\dot{x}_{1,N} + \\ &\quad \frac{\partial h(x,u)}{\partial x_{2,1}}\dot{x}_{2,1} + \ldots + \frac{\partial h(x,u)}{\partial x_{2,N}}\dot{x}_{2,N} + \\ &\quad \frac{\partial h(x,u)}{\partial u}\dot{u} \\ &= \begin{bmatrix} \frac{\partial h(x,u)}{\partial x_{1,1}} & \ldots & \frac{\partial h(x,u)}{\partial x_{2,N}} \end{bmatrix}\dot{x} + \frac{\partial h(x,u)}{\partial u}\dot{u} \\ &= \begin{bmatrix} \frac{\partial L_f^0(h)}{\partial x_{1,1}} & \ldots & \frac{\partial L_f^0(h)}{\partial x_{2,N}} \end{bmatrix}(Ax+Bu) + \frac{\partial L_f^0(h)}{\partial u}\dot{u}. \end{aligned} \tag{16}$$

The general case of $n-1^{th}$ Lie derivative produces

$$\begin{aligned} L_f^{n-1}(h) &= \begin{bmatrix} \frac{\partial L_f^{n-2}(h)}{\partial x_{1,1}} & \ldots & \frac{\partial L_f^{n-2}(h)}{\partial x_{2,N}} \end{bmatrix}(Ax+Bu) + \\ &\quad \frac{\partial L_f^{n-2}(h)}{\partial u}\dot{u} + \ldots + \frac{\partial L_f^{n-2}(h)}{\partial u}\dot{u}^{n-1}. \end{aligned} \tag{17}$$

The observability matrix is constructed as the gradient with respect to the state vector x of the above Lie derivatives, given by

$$\mathcal{O} = \frac{d}{dx}\begin{bmatrix} L_f^0(h) \\ L_f^1(h) \\ \vdots \\ L_f^{n-1}(h) \end{bmatrix} = \begin{bmatrix} \frac{\partial L_f^0(h)}{\partial x_1} & \ldots & \frac{\partial L_f^0(h)}{\partial x_n} \\ \vdots & \ddots & \vdots \\ \frac{\partial L_f^{n-1}(h)}{\partial x_1} & \ldots & \frac{\partial L_f^{n-1}(h)}{\partial x_n} \end{bmatrix}. \tag{18}$$

It follows that if $rank(\mathcal{O}) = n$, evaluated for all values x_0 in the state space trajectory, then the SPM is considered weakly locally observable. Moreover, the condition number of the observability matrix $\mathcal{O}$ will inform and quantify the quality of the concentration estimates at any given operating point x_0.

VI. RESULTS AND DISCUSSION

The SPM observability matrix for the estimation of lithium concentration in both electrodes from the input and output measurements is given in (18). This section not only aims at evaluating the observability of the SPM, but, more importantly, aims to understand the practical aspects of developing an observer by evaluating the observability matrix under different electrode chemistry nonlinearities, different input conditions, and varying discretization grid points. The following results are specifically for a lithium-ion cell with Graphite at the negative electrode and Lithium Nickel Manganese Cobalt Oxide (NMC) at the positive electrode, unless specified otherwise. Note that the observability matrix and condition number tests are evaluated at all possible points in the state space trajectory, under the specified input condition.

A. NONLINEAR VS. LINEARIZED OBSERVABILITY ANALYSIS

For nonlinear systems, the observability is defined in terms of indistinguishability of states at every operating point x_0 with respect to the inputs. In essence, the observability property of nonlinear systems also depends on the input, as opposed to the analysis for linearized systems that exclusively depends on the system matrix and the output distribution matrix. Neglecting the effect of input renders the observability analysis on linearized systems to be incorrect and incomplete.

A SPM with $x \in \mathbb{R}^n$ where $n = 6$ is subjected to a constant discharge current of 1C. The observability matrix rank and condition number from the nonlinear and linearized observability (wherein the observability matrix is constructed on a linearized SPM) analyses are compared in Fig. 2. For both cases, it is observed that the observability matrix at all possible points in the state space trajectory (in terms of SOC) remains full rank, but the condition number is many orders of magnitude higher in the linearized analysis case, clearly indicating that the linearized observability matrix is close to being singular and losing rank. On the other hand, the nonlinear analysis with its inherent dependence on input and its derivatives exhibits a higher condition number, thereby providing a true picture of SPM's observability.

B. DEPENDENCE ON INPUT CURRENT

The observability property of the SPM needs to be understood in the presence and absence of current input. A SPM with $x \in \mathbb{R}^n$ where $n = 6$ is subjected to a zero input and different constant discharge current (1, 3, and 5C) conditions. For each case, it is observed that the observability matrix at all possible points in the state space trajectory (in terms of SOC) remains full rank as shown in Fig. 3.a, however, the condition number is very high in the absence of current as witnessed in Fig. 3.b and also increases as the magnitude of current decreases. This highlights the primary difficulty with using SPM-based observers to estimate the concentration in both electrodes. At steady-state, when the battery is at rest, a single terminal voltage measurement is available at every time step, which is to be used to estimate the open circuit potential of the electrodes. There is no unique combination of the electrode open circuit potentials that gives the exact terminal voltage. Hence, the higher condition number at steady state highlights this intrinsic challenge of estimating individual electrode potential, and by extension, individual electrode concentrations. Having said that, it is to be noted that in the cases where input current is non-zero (for 1, 3, and 5C cases), the condition number is still fairly high

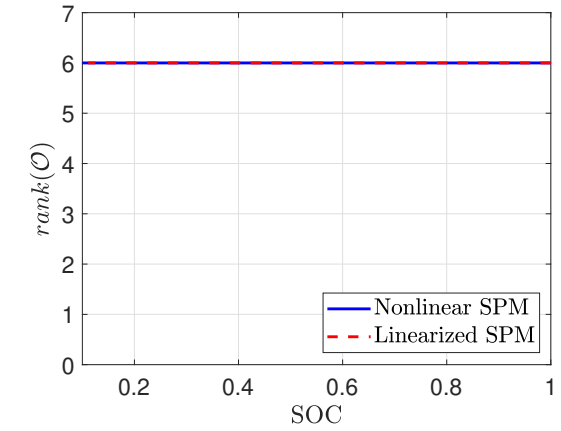

(a)

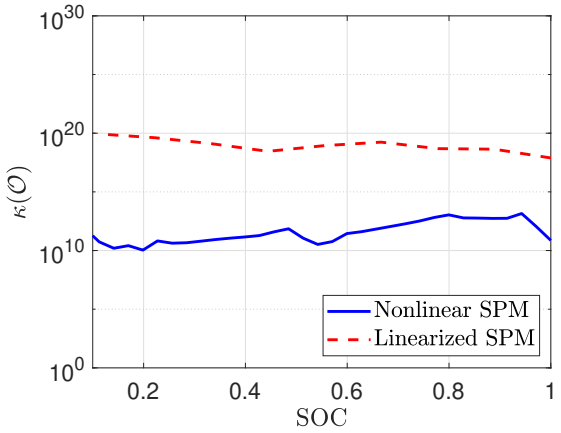

(b)

FIGURE 2: Comparison between nonlinear and linearized observability analysis for a SPM with $n = 6$ states under a nominal discharge current of 1C. The rank test of the observability matrix is in (a) and the condition number in (b).

(approximately 10^{10}), which indicates that the accuracy of the lithium concentration estimates in both electrodes are poor.

C. DEPENDENCE ON DISCRETIZATION GRIDS AT STEADY STATE

Next, one of the practical aspects of developing a SPM-based observer is to select the discretization grid points (N, recall $n = 2N$) while converting the original PDE battery dynamics into a system of ODEs, such that the computational complexity and model fidelity is compromised. To that end, the rank of the observability matrix is evaluated for three cases of (i) $n = 4$, (ii) $n = 6$, and (iii) $n = 8$ at all possible points in the state space trajectory. At steady state, when the input current is zero ($u = I_{batt} = 0$), the lower bound for the grid size is ascertained. In Fig. 3.c, it is evident that with $n = 4$ that the observability matrix loses rank (rank is 3 instead of 4) making the SPM not observable. This is attributed to the fact that the reduced-order SPM ($n = 4$) has truncated dynamics, which prevents to accurately capture the battery dynamics, making it unsuitable for observer design. Hence, a SPM with $n \geq 6$ that captures more dynamics (via states), and hence more information, will ensure the observability matrix to hold a full rank. However, increasing the discretization grid points ($n \geq 6$) does not directly translate to better observability. In Fig. 3.d, the condition number of the observability matrix is evaluated for three cases of (i) $n = 4$, (ii) $n = 6$, and (iii) $n = 8$ under a constant discharge current of 1C. It is observed that as the discretization grid points increase, the condition number increases by a couple of orders of magnitude, thus making it not preferable for observer design. Thus, there is a trade-off to be considered when selecting the number of discretization grid points, wherein increasing grid points ($n \geq 6$) increases the condition number but at the same time going low ($n = 4$) makes the observability matrix lose rank.

D. DEPENDENCE ON POSITIVE ELECTRODE CHEMISTRY

To generalize the nonlinear observability analysis for a SPM, it is critical to investigate how the SPM-based observer will function for different positive electrode's chemistry in the family of lithium-ion batteries. Assuming that the negative electrode is always Graphite, the observability matrix is evaluated for NMC, Lithium Manganese Oxide (LMO), and Lithium Iron Phosphate (LFP). It is to be noted that the gradient of the positive electrode's open circuit potential curves, which constitute the nonlinearities in the output voltage equation of the SPM, are major contributors in determining the rank and condition number of the observability matrix. For a SPM with $n = 6$ under a constant discharge current of 1C, the rank and condition number analyses are shown in Fig. 3.d and 3.e, respectively. The plots highlight that the observability matrix does not lose rank, however, the condition number of LFP is orders of magnitude higher than that of NMC and LMO. This is attributed to the flat open circuit potential of LFP due to the two-phase region, thereby making the gradients of the potential with respect to the concentration to be close to zero. The flatness results in an ill conditioned observability matrix with a higher condition number.

E. OBSERVABILITY ISSUES AND SOLUTIONS

Clearly, from the aforepresented results, the observability of the SPM while estimating the lithium concentration in both electrodes, is riddled with dependencies on various factors such as input current, discretization grids, positive electrode's chemistry. Moreover, it is observed nonlinear observability analysis is more complete and informative than a linearized one. And finally, in every case seen thus far, the observability matrix has a very high condition number $\left(\geq 10^{10}\right)$, which translates to poor estimation accuracy. This signifies that an observer designed to estimate the concentration in both

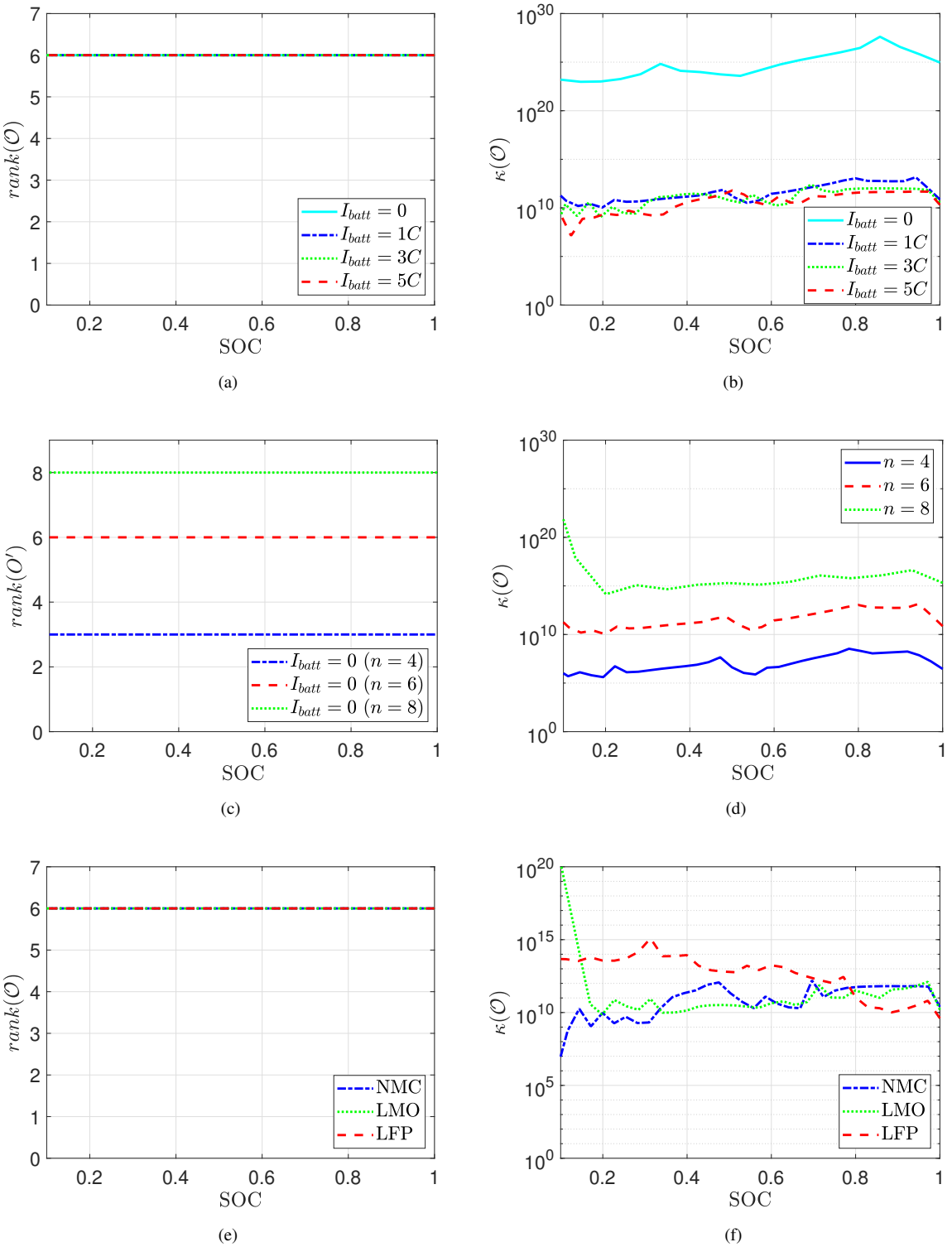

FIGURE 3: Effect of input current (0C, 1C, 3C, and 5C) on the observability matrix (a) rank and (b) condition number for a SPM with $n = 6$ states. Dependency of observability matrix's rank on discretization grid points for SPM with $n = 4$ and $n = 6$ states at steady state in (c), and dependency of observability matrix's condition number on discretization grids for SPM with $n = 4$, $n = 6$, and $n = 8$ states under a nominal current of 1C in (d). Effect of electrode's chemistry on the observability matrix (e) rank and (f) condition number for a SPM with $n = 6$ states under a nominal current of 1C.

electrodes, henceforth referred to as the observer for both electrodes, from the available current and voltage measurements will provide inaccurate results. Owing to this, the literature has proposed different observer schematics to overcome this issue. Some observers are designed by assuming lithium conservation and enforcing an algebraic relationship between the lithium concentration of the two electrodes [9], [14], which reduces the estimation problem down to only estimating the concentration in one electrode, thereby improving the condition number of the observability matrix. Another class of observers are designed for individual electrodes like the single electrode observer [12] and the interconnected observer [16], [17] that estimate the concentration in one electrode in closed-loop and simulate the concentration of the other electrode in open-loop. By choosing an electrode-level observer structure, the condition number of the observability matrix is improved since the concentration in only one electrode is to be estimated. This subsection aims to quantify the improvement in the condition number of the observability matrix brought about by choosing an observer structure, such as the interconnected observer, by comparing it with the observer for both electrodes seen in Sections VI-A - VI-D.

The interconnected observer [16], [17] contains a dedicated observer for each electrode (positive electrode observer and negative electrode observer) to circumvent the observability issues (of estimating concentration in both electrodes) with a bidirectional interconnection structure to enable concurrent estimation of lithium concentration in either electrodes. Following the nonlinear observability analysis outlined in (5) for the positive and negative electrode observer, the condition number of the respective observability matrices is shown alongside the condition number of the observer for both electrodes (under a constant current discharge of 1C) in Fig. 4. As observed, a significant improvement is noticed through the usage of an interconnected observer structure, wherein the condition number for the positive and negative electrode observers are many orders of magnitude lower (by at least 10^5) than the observer for both electrodes. Note that the condition number for the positive electrode observer is lower than the negative electrode observer due to the steep curve of the NMC open circuit potential as opposed to the more flatter open circuit potential of the Graphite.

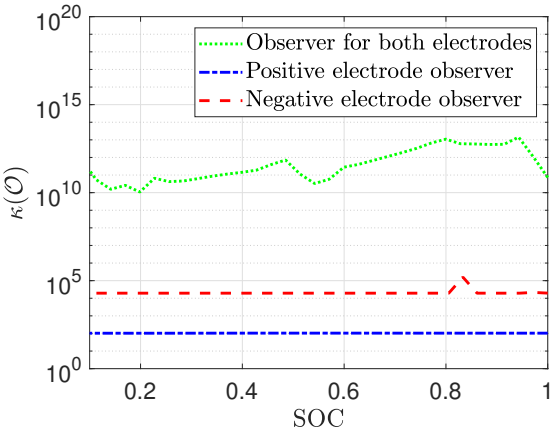

FIGURE 4: The condition number of the positive and negative electrode observer (from the intrerconnected observer structure) compared to the observer for both electrodes.

VII. IMPACT AND OUTLOOK

The nonlinear observability analysis presented in this paper has been spurred from an interactive and thought-provoking discussion among researchers in the field of battery control and estimation at the *Advanced Battery Management* workshop held during the 59^{th} *IEEE Control Decision Conference, 2020*. This paper provides a systematic framework to evaluate the observability of a nonlinear electrochemcial model under different conditions (inputs, grid sizes, positive electrode's chemistry) and aid the synthesis of a model-based observer. The substantial impact of the work includes

1) stressing the need for nonlinear observability analysis instead of a linearized observability analysis. The common practice of linearized observability analysis does not respect the nonlinearities of the system and neither does it account for the input current and its derivatives, thereby leading to an incomplete and incorrect analysis, as far as the observability property of the system is concerned,
2) demonstrating that a complete nonlinear observability analysis can only be carried out by quantifying the measure of observability by accounting for the rank and the condition number of the observability matrix,
3) emphasizing that the observability property of the electrochemical model depends on different conditions such as the input current profile, electrode's chemistry, and discretization grid points, which informs the synthesis of the structure and design of a model-based observer.

Further, the framework for nonlinear observability analysis for SPM laid out in this work can be extended to assess the parameter identifiability of the SPM. It is to be noted that the nonlinear battery electrochemical model (SPM) is highly over-parameterized, which poses a problem during parameter identification and motivates the need to carry out parameter identifiability [26] of the model to assess whether the parameters can be identified from the available measurements. However, by reformulating the model parameters as constant state variables, an augmented state vector is created and the differential geometry approach outlined in Section V can be adopted to recast the parameter identifiability problem as an observability analysis problem [27]. This is particularly also important in determining the subset of model parameters that are identifiable or observable as the battery ages, which can be harnessed for developing battery health estimation algorithms. In essence, the nonlinear observability analysis framework presented in this work can be easily extended to parameter identifiability studies.

Moreover, this work brings to light an outlook that is lacking in the process of electrochemical model-observer design. The work highlights that the order of the electrochemical model used in the observer is a trade-off between lower condition number (better observability) and model accuracy. As the model order increases, the condition number increases exponentially, however, a decrease in model order introduces modeling errors due to truncating or neglecting higher order dynamics. This results in a model-based observer that may not estimate state accurately since the underlying model is not the best approximation of the real system. This begs the need for robust observers that account for the modeling errors in the form of uncertainties during observer synthesis.

VIII. CONCLUSION

In this work, a nonlinear observability analysis of a battery electrochemical model is presented by accounting for the rank and condition number of the observability matrix under different conditions, ranging from different inputs and grid sizes to positive electrode's chemistry. The results confirm that a nonlinear observability analysis is more complete since a linearized analysis fails to respect the nonlinearities of the system. Further, the results provide guidelines for a proper observer design for nonlinear battery electrochemical models.

REFERENCES

[1] N. A. Chaturvedi, R. Klein, J. Christensen, J. Ahmed, and A. Kojic, "Algorithms for advanced battery-management systems," *IEEE Control systems magazine*, vol. 30, no. 3, pp. 49–68, 2010.

[2] L. Lu, X. Han, J. Li, J. Hua, and M. Ouyang, "A review on the key issues for lithium-ion battery management in electric vehicles," *Journal of power sources*, vol. 226, pp. 272–288, 2013.

[3] M. A. Hannan, M. H. Lipu, A. Hussain, and A. Mohamed, "A review of lithium-ion battery state of charge estimation and management system in electric vehicle applications: Challenges and recommendations," *Renewable and Sustainable Energy Reviews*, vol. 78, pp. 834–854, 2017.

[4] R. Xiong, L. Li, and J. Tian, "Towards a smarter battery management system: A critical review on battery state of health monitoring methods," *Journal of Power Sources*, vol. 405, pp. 18–29, 2018.

[5] D. N. How, M. Hannan, M. H. Lipu, and P. J. Ker, "State of charge estimation for lithium-ion batteries using model-based and data-driven methods: A review," *Ieee Access*, vol. 7, pp. 136 116–136 136, 2019.

[6] G. L. Plett, "Extended kalman filtering for battery management systems of lipb-based hev battery packs: Part 3. state and parameter estimation," *Journal of Power sources*, vol. 134, no. 2, pp. 277–292, 2004.

[7] I.-S. Kim, "The novel state of charge estimation method for lithium battery using sliding mode observer," *Journal of Power Sources*, vol. 163, no. 1, pp. 584–590, 2006.

[8] S. Santhanagopalan and R. E. White, "State of charge estimation using an unscented filter for high power lithium ion cells," *International Journal of Energy Research*, vol. 34, no. 2, pp. 152–163, 2010.

[9] D. Di Domenico, A. Stefanopoulou, and G. Fiengo, "Lithium-ion battery state of charge and critical surface charge estimation using an electrochemical model-based extended kalman filter," *Journal of dynamic systems, measurement, and control*, vol. 132, no. 6, 2010.

[10] T. R. Tanim, C. D. Rahn, and C.-Y. Wang, "State of charge estimation of a lithium ion cell based on a temperature dependent and electrolyte enhanced single particle model," *Energy*, vol. 80, pp. 731–739, 2015.

[11] R. Ahmed, M. El Sayed, I. Arasaratnam, J. Tjong, and S. Habibi, "Reduced-order electrochemical model parameters identification and state of charge estimation for healthy and aged li-ion batteries Part II: Aged battery model and state of charge estimation," *IEEE Trans. Emerg. Sel. Topics Power Electron.*, vol. 2, no. 3, pp. 678–690, 2014.

[12] A. Bartlett, J. Marcicki, S. Onori, G. Rizzoni, X. G. Yang, and T. Miller, "Electrochemical model-based state of charge and capacity estimation for a composite electrode lithium-ion battery," *IEEE Trans. Control Syst. Technol.*, vol. 24, no. 2, pp. 384–399, 2016.

[13] N. Lotfi, R. G. Landers, J. Li, and J. Park, "Reduced-order electrochemical model-based soc observer with output model uncertainty estimation," *IEEE Transactions on Control Systems Technology*, vol. 25, no. 4, pp. 1217–1230, 2016.

[14] S. J. Moura, F. B. Argomedo, R. Klein, A. Mirtabatabaei, and M. Krstic, "Battery state estimation for a single particle model with electrolyte dynamics," *IEEE Trans. Control Syst. Technol.*, vol. 25, no. 2, pp. 453–468, 2017.

[15] S. Dey and B. Ayalew, "Real-time estimation of lithium-ion concentration in both electrodes of a lithium-ion battery cell utilizing electrochemical–thermal coupling," *Journal of Dynamic Systems, Measurement, and Control*, vol. 139, no. 3, p. 031007, 2017.

[16] A. Allam and S. Onori, "An interconnected observer for concurrent estimation of bulk and surface concentration in the cathode and anode of a lithium-ion battery," *IEEE Transactions on Industrial Electronics*, vol. 65, no. 9, pp. 7311–7321, 2018.

[17] A. Allam and S. Onori, "On-line capacity estimation for lithium-ion battery cells via an electrochemical model-based adaptive interconnected observer," *IEEE Transactions on Control Systems Technology*, vol. 29, no. 4, 2021.

[18] A. Allam, E. Catenaro, and S. Onori, "Pushing the envelope in battery estimation algorithms," *Iscience*, vol. 23, no. 12, p. 101847, 2020.

[19] D. Zhang, L. D. Couto, and S. J. Moura, "Electrode-level state estimation in lithium-ion batteries via kalman decomposition," *IEEE Control Systems Letters*, vol. 5, no. 5, pp. 1657–1662, 2020.

[20] S. Zhao, S. R. Duncan, and D. A. Howey, "Observability analysis and state estimation of lithium-ion batteries in the presence of sensor biases," *IEEE Transactions on Control Systems Technology*, vol. 25, no. 1, pp. 326–333, 2016.

[21] R. Hermann and A. Krener, "Nonlinear controllability and observability," *IEEE Transactions on automatic control*, vol. 22, no. 5, pp. 728–740, 1977.

[22] K. W. Lee, W. S. Wijesoma, and J. I. Guzman, "On the observability and observability analysis of slam," in *2006 IEEE/RSJ International Conference on Intelligent Robots and Systems*. IEEE, 2006, pp. 3569–3574.

[23] J. Wilson and S. Guhe, "Observability matrix condition number in design of measurement strategies," in *Computer Aided Chemical Engineering*. Elsevier, 2005, vol. 20, pp. 397–402.

[24] A. J. Krener and K. Ide, "Measures of unobservability," in *Proceedings of the 48h IEEE Conference on Decision and Control (CDC) held jointly with 2009 28th Chinese Control Conference*. IEEE, 2009, pp. 6401–6406.

[25] S. Zeng, "Observability measures for nonlinear systems," in *2018 IEEE Conference on Decision and Control (CDC)*. IEEE, 2018, pp. 4668–4673.

[26] R. Bellman and K. J. Åström, "On structural identifiability," *Mathematical biosciences*, vol. 7, no. 3-4, pp. 329–339, 1970.

[27] E. Tunali and T.-J. Tarn, "New results for identifiability of nonlinear systems," *IEEE Transactions on Automatic Control*, vol. 32, no. 2, pp. 146–154, 1987.

ANIRUDH ALLAM (Graduate Student Member, IEEE) received the B.E. degree in electronics and telecommunication engineering from the University of Pune, Pune, India, in 2010, and the M.S. degree in automotive engineering from Clemson University, Clemson, SC, USA, in 2015. He is currently pursuing the Ph.D. degree with the Department of Energy Resources Engineering, Stanford University, Stanford, CA, USA.

His research interests include estimation, control, and degradation modeling of electrochemical energy storage systems.

SIMONA ONORI (Senior Member, IEEE) received the Laurea degree in computer science and engineering from the University of Rome "Tor Vergata" Rome, Italy, in 2003, the M.S. degree in electronics and communications engineering from The University of New Mexico, Albuquerque, NM, USA, in 2005, and the Ph.D. degree in control engineering from the University of Rome "Tor Vergata" in 2007.

She is currently an Assistant Professor with the Energy Resources Engineering Department, Stanford University, Stanford, CA, USA. Her research focuses on modeling and control in sustainable transportation, clean energy, and secondary life battery areas.

Dr. Onori is the recipient of the 2020 U.S. DOE C3E Award in the research category, the 2019 Board of Trustees Award for Excellence, Clemson University, the 2018 Global Innovation Contest Award from LG Chem, the 2018 SAE Ralph R. Teetor Educational Award, and the 2017 NSF CAREER Award. She has been serving as the Editor-in-Chief for the SAE International Journal of Electrified Vehicles since 2020. She is a Distinguished Lecturer of the IEEE Vehicular Technology Society.